

1 **Simulated solar photo-assisted decomposition of peroxymonosulfate. Radiation**
2 **filtering and operational variables influence on the oxidation of aqueous bezafibrate**

3 Rafael R. Solís^{1,2,3,*}, F. Javier Rivas^{1,2,*}, Ana M. Chávez^{1,2}, Dionysios D. Dionysiou³

4 ¹Departamento de Ingeniería Química y Química Física, Universidad de Extremadura.
5 Avda. Elvas s/n, 06006 Badajoz (Spain)

6 ²Instituto Universitario del Agua, Cambio Climático y Sostenibilidad (IACYS),
7 Universidad de Extremadura, Avda. de la Investigación s/n, 06006 Badajoz (Spain)

8 ³Environmental Engineering and Science Program, Department of Chemical and
9 Environmental Engineering, College of Engineering & Environmental Science (CEAS),
10 Engineering Research Center (ERC), University of Cincinnati. 2901 Woodside Dr.,
11 Cincinnati OH 45221-0012 (USA)

12 *Correspondence to Rafael Rodríguez Solís (rrodrig@unex.es; rodrigr2@ucmail.uc.edu),
13 Francisco Javier Rivas (fjrivias@unex.es)

14 **Abstract**

15 This work investigates the potential of the combination of peroxymonosulfate (PMS)
16 and simulated solar radiation ($\lambda > 300$ nm) to remove bezafibrate from aqueous solution.
17 Different solar light filters indicate a higher removal efficiency as the wavelength range
18 used moves to the more energetic region of the solar spectrum. The system PMS/Daylight
19 (300-800 nm) eliminates bezafibrate (1 mg L^{-1}) in less than 30 min under the best
20 conditions used in this study ($C_{\text{PMS}} = 4 \cdot 10^{-4} \text{ M}$) with no pH control (acidic pH). The
21 efficiency of the process significantly improves under alkaline conditions (pH=10), likely
22 due to a higher PMS photolysis rate. Experiments conducted at different initial
23 concentration of PMS and bezafibrate suggest first order regarding PMS and different
24 from 1 in the case of bezafibrate. Intermediates generated at the beginning of the process

1 have been tentatively identified to propose a hypothetical reaction pathway and to
2 estimate their toxicity.

3 **Keywords:** peroxymonosulfate, simulated solar radiation, bezafibrate, intermediates

4 1. INTRODUCTION

5 Pharmaceutical compounds are substances that, after undergoing strict manufacturing
6 processes and rigorous clinical studies, are commercialized to confer a benefit to human
7 health. Revenues of the world pharmaceutical industry market have exceeded the 1100
8 billion USD in the last years, giving an idea of the immensity of this manufacturing
9 industry (STATISTA, 2018). As a consequence, due to the high and in many cases
10 abusive use of these compounds, pharmaceutical substances are often found in
11 environments far away from the production locations. Actually, they can enter the aquatic
12 environment by excretion of non-metabolized active ingredients by direct disposal to
13 public sewage (Razavi et al., 2009).

14 Fibric acid derivatives (fibrates), such as bezafibrate (BZF), are a class of medication
15 that lowers blood triglyceride levels (Jones, 2009). Fibrates can be classified as
16 persistent/recalcitrant according to the European Union criteria for soil and sediments
17 (EU, 2003). Moreover, aerobic activated sludge processes have reported to be inefficient
18 in the oxidation of BZF (Sui et al., 2016). Bezafibrate has been found in water bodies at
19 $\mu\text{g L}^{-1}$ levels (Daughton and Ternes, 1999). Accordingly, efficient, cost-effective, and
20 environmentally sustainable technologies aimed at reducing pharmaceuticals in water
21 bodies are of high interest, especially if water is reused (Christou et al., 2017).

22 The use of solar radiation in combination with inorganic peroxides can be an efficient
23 alternative in the treatment of recalcitrant contaminants found at low concentrations.
24 Potassium peroxymonosulfate (PMS) has recently attracted attention in the field of water

1 treatment as an oxidizing agent characterized by some attractive characteristics, including
2 easy handling. In solution, PMS can directly oxidize organic and inorganic compounds;
3 or, alternatively, can be decomposed into radicals after activation mainly with catalysts,
4 radiation, or heat (Solís et al., 2016). Use of radiation is an attractive option since no
5 additional chemicals are added to water. Most of referenced works use UVC radiation to
6 activate PMS (Ghanbari and Moradi, 2017; Wang and Wang, 2018); however, more
7 economic radiation sources would result in a significant decrease in operating costs. Solar
8 radiation is an interesting source since the spectrum starts at wavelengths as low as 290-
9 300 nm (Beltrán and Rey, 2017). PMS decomposition at $\lambda > 300$ nm would eventually lead
10 to an inexpensive and efficient oxidation if compared to traditional UV sources.

11 Accordingly, in this work bezafibrate has been treated in the presence of PMS with
12 solar simulated radiation. Solar simulated radiation and the use of filters allow for the
13 selection of the radiation wavelength range, keeping the reaction conditions under control
14 to assess the impact of different operating parameters. Intermediates generated at the
15 beginning of the process have been tentatively identified to propose a hypothetical
16 reaction pathway and to estimate their toxicity.

17 **2. EXPERIMENTAL SECTION**

18 **2.1. Chemicals**

19 Bezafibrate (BZF, $C_{19}H_{20}ClNO_4$, CAS: 41859-67-0) was of analytical standard grade
20 (>99%) and was purchased from Sigma-Aldrich®. Peroxymonosulfate (PMS) technical-
21 grade was acquired as Oxone® compound from Sigma-Aldrich®
22 ($2KHSO_5 \cdot KHSO_4 \cdot K_2SO_4$, CAS: 37222-66-5). The rest of chemicals were of analytical
23 grade and were purchased from Panreac®. All test and store solutions were prepared with
24 ultrapure water from a Milli-Q® Integral 5 system (18.2 M Ω cm). HPLC-grade

1 acetonitrile was used for analytical HPLC analysis, and LC-MS-grade acetonitrile for LC-
2 QTOF-MS determinations.

3 **2.2. Experimental installation and procedure**

4 Solar PMS decomposition was conducted in a Suntest CPS+ simulator (Atlas, Illinois,
5 USA) in which a 500 mL borosilicate glass beaker was placed, under magnetic stirring.
6 The emitted simulated solar radiation was restricted to different ranges by using filters:
7 Daylight (300-800 nm), Windowglass (320-800 nm), Storelight (360-800 nm) and Visible
8 (390-800 nm). The radiation intensity reaching the surface and bottom of the reactor (see
9 graphical abstract) were measured with the help of a BLACK-Comet UV-visible
10 spectroradiometer (StellarNet Inc., Florida, USA). Table 1 shows the global intensity
11 irradiance values and the percentages of each component (UVC, UVB, UVA and visible)
12 in each case measured in the liquid surface and bottom of the reactor (see points A and B
13 in graphical abstract). The radiation intensity absorbed by the aqueous media was
14 quantified by means of the reduction of ferrioxalate complex actinometry (Goldstein and
15 Rabani, 2008). For that purpose, actinometry tests were conducted in the presence of
16 oxalic acid 45 mM and iron perchlorate (Fe^{3+} , 15 mM) in perchloric acid (30 mM) at
17 pH=2. Oxygen interference was suppressed by bubbling nitrogen during the course of the
18 test. The reduced iron (II) was photometrically analyzed by complexation with 1,10-
19 phenanthroline (Tamura et al., 1974).

20 Experiments were carried out by adding the required amount of PMS dissolved in 10
21 mL of water to 500 mL of aqueous bezafibrate solution. The range of PMS concentration
22 in this study was within the range $8 \cdot 10^{-4}$ - $4 \cdot 10^{-5}$ M. In order to maintain experimental
23 analytical errors in HPLC to a minimum, an abnormal high concentration of bezafibrate
24 was used (in the range of 1.1-11.5 mg L⁻¹; ~1 mg L⁻¹, typically). The identification of

1 intermediate oxidation products was carried out in experiments with higher initial BZF
2 concentration in ultrapure water, i.e. $\sim 10 \text{ mg L}^{-1}$, to ensure their generation in enough
3 concentration to appreciate the signal during HPLC-QTOF analysis. Before starting, the
4 initial control sample was extracted and irradiation of the solution began by switching on
5 the solar simulator after PMS addition. At different predetermined time intervals, samples
6 were taken for analyses. pH was controlled, when required, by adding H_3PO_4 to reach 10
7 mM in the media and raised to the desired value with NaOH solution. In order to stop the
8 reaction, samples were quenched by adding 10 μL of sodium thiosulfate 0.1 M.

9 Synthetic urban wastewater simulating a biological treated effluent was prepared
10 according to a literature recipe (Erdei et al., 2008). Table 2 shows the composition and
11 properties of the effluent. BZF was added to the mixture from a concentrated solution to
12 obtain a final concentration of $250 \mu\text{g L}^{-1}$. pH was unaltered.

13 **2.3. Aqueous analyses**

14 Aqueous concentration of bezafibrate was determined by Liquid Chromatography
15 (LC) in a HPLC with Diode-Array detection. The apparatus used was an UFLC Shimadzu
16 Prominence LC-AD. A flow rate of 0.5 mL min^{-1} mobile phase was pumped at a ratio of
17 50:50 mixture of acetonitrile and acidified water (0.1% of H_3PO_4). The column stationary
18 phase was core-shell C18 Kinetex® (150 x 4.6 mm, particle size $5 \mu\text{m}$ & pore 100 \AA) and
19 was thermally maintained at $30 \text{ }^\circ\text{C}$. Quantification of bezafibrate was conducted at 227
20 nm.

21 First intermediates generated in the system PMS/Daylight were tentatively identified
22 by HPLC coupled to a Quadrupole Time of Flight (HPLC-QTOF) instrument. As a rule
23 of thumb, 5 μL of sample of the reacting mixture was injected in an Agilent 1260 HPLC
24 coupled to an Agilent 6520 Accurate Mass QTOF LC/MS. A Zorbax Eclipse Plus C18
25 column ($3.5 \mu\text{m}$, $4.6 \times 100 \text{ mm}$), thermally maintained at $30 \text{ }^\circ\text{C}$, was used as stationary

1 phase. The mobile phase consisted of a mixture of pure MilliQ® water (phase A) and
2 acetonitrile (phase B), fed at a flow rate of 0.4 mL min⁻¹. The following gradient was
3 applied: A:B with a 90:10 ratio for 2 min and raised to 10:90 in 23 min, and maintained
4 for 2 min for equilibration. The QTOF conditions were: ESI (-) mode, gas temperature
5 325 °C, drying gas 10 mL min⁻¹, nebulization 45 psig, Vcap 3500 V, fragmentation 100
6 V, acquisition m/z range 100-1000. MS spectra were processed by an Agilent Mass
7 Hunter Qualitative Analysis B.04.00 software. Potential candidates for intermediates and
8 the oxidation route were proposed following some *in silico* tools guidance such as the
9 University of Minnesota Pathway Prediction System (UM-PPS) and PathPred (Bletsou et
10 al., 2015). The transformation products reported for bezafibrate oxidation during other
11 Advanced Oxidation Processes technologies were also taken into account.

12 Inorganic and short-chain organic acids were determined by an Ion Chromatograph
13 (IC) coupled to a conductivity detector. A Methrom® 881 Compact IC pro equipped with
14 chemical suppression, 863 Compact autosampler, and anionic-exchange column
15 (MetroSep A sup 5, 250x4.0 mm, particles of 5 µm) thermally maintained at 45 °C was
16 used. The used mobile phase program consisted of a 0.7 mL min⁻¹ gradient of aqueous
17 Na₂CO₃ from 0.6 mM to 14.6 mM in 50 min.

18 Total Organic Carbon was determined in a TOC-V_{CSH} (Shimadzu®) analyzer whose
19 analysis is based on catalytic combustion and Non-Dispersive InfraRed (NDIR)
20 detection.

21 Concentration of peroxymonosulfate (PMS) was determined by a spectrophotometric
22 method based on N,N-diethyl-phenylenediamine (DPD) oxidation (Fukushima and
23 Tatsumi, 2005).

1 pH was measured in a Basic 20 pHmeter of Crison® equipped with a 50 11T electrode,
2 conductivity in a Crison® 524 device, and turbidity in a 2100 IS Hach® apparatus.

3 3. RESULTS AND DISCUSSION

4 3.1. Preliminary experiments.

5 Before proceeding with the PMS/radiation experiments, some control runs were
6 carried out to ascertain the extent of the direct BZF oxidation by peroxymonosulfate, the
7 influence of radiation nature and the role played by the irradiated area. Fig. 1A shows the
8 capability of PMS to directly oxidize bezafibrate as a function of pH. As seen from this
9 figure, an increase of pH from 3 to 7 leads to a higher oxidation extent, suggesting an
10 enhanced reactivity of the anionic form of bezafibrate. Thus, the pK_a value for BZF is 3.6
11 (Fent et al., 2006), sustaining the previous hypothesis. However, when pH was further
12 raised to 9, the process was partially inhibited, likely due to the second dissociation of
13 PMS leading to the less reactive SO₅²⁻ (pK_a=9.5). Additionally, at high pH, PMS can self-
14 decompose to oxygen and sulfate through a non-radical route (Liu et al., 2015).

15 The process is supposed to follow second order kinetics. A first approach to the second
16 order rate constant (k_{Direct}) can be attempted by adjusting experimental PMS
17 concentration to a mathematical time dependent expression and solving by Euler's
18 method:

$$19 \quad C_{\text{BZF}}^{t+1} = C_{\text{BZF}}^t - \left(k_{\text{Direct}} C_{\text{PMS}}^t C_{\text{BZF}}^t \right) (\Delta t) \quad (1)$$

20 where C_i^t refers to concentration of species i at time t, and Δt is the time increment used
21 in the numerical method.

1 Approximated values of 0.08 ± 0.01 , 0.29 ± 0.03 and $0.16\pm 0.02 \text{ M}^{-1} \text{ s}^{-1}$ for k_{Direct} where
2 obtained when initial pH values were adjusted to 5, 7, and 9, respectively. At pH 3, BZF
3 elimination was completely inhibited.

4 Next, uncontrolled pH runs were conducted in the presence of radiation of different
5 nature. Fig. 1B shows the influence of the wavelength applied when BZF was oxidized
6 after addition of PMS. As observed from this figure, as the radiation is more energetic
7 (lower wavelength) the efficacy of the system PMS/radiation increases in terms of
8 bezafibrate abatement (Matafonova and Batoev, 2018). Hence, after one hour of
9 treatment, BZF conversion values of 0, 20, 60 and 97% were found in the systems PMS,
10 PMS/Storelight, PMS/Windowsglass, and PMS/Daylight, respectively, when $2 \cdot 10^{-4} \text{ M}$ in
11 PMS initial concentration was used. At the conditions applied in this series, bezafibrate
12 is not directly oxidized nor photolyzed. Accordingly, the significant enhancement of the
13 process in the presence of peroxymonosulfate is undoubtedly due to PMS
14 disproportionation because of the presence of UV radiation (Wacławek et al., 2017; Wang
15 and Wang, 2018). Having in mind the low radiation absorption coefficient of PMS at
16 $\lambda > 280 \text{ nm}$ (Ao and Liu, 2017), shown in Fig. 2, it is suggested that the disproportionation
17 quantum yield must be significant.

18 Finally, the process was tested to check the influence of area radiation exposure. Fig.
19 1C reveals a significant role played by the irradiated area. As expected, the higher the
20 exposure area, the higher the BZF elimination rate.

21 Given the results obtained in this section, next experiments were conducted in the
22 presence of PMS and daylight.

3.2. Influence of operation variables

3.2.1. Initial bezafibrate concentration

The influence of initial bezafibrate concentration was assessed in the interval $3 \cdot 10^{-6}$ to $3 \cdot 10^{-5}$ M. Fig. 3A shows the results obtained. As inferred from this figure, initial BZF concentration influence reveals a kinetic behavior different from the traditional first order, commonly applied to advanced oxidation processes. A rough analysis of the reaction rate at time zero confirms that the higher the initial parent compound concentration, the higher the reaction rate. A simple pseudo-first order kinetics does not explain the BZF concentration profile monitored. Accordingly, a more complicated mechanism must proceed. The actual mechanism of the BZF/PMS/Daylight system is complex, including the radiation transfer equation, sulfate and/or hydroxyl radical generation, propagation and termination of radicals, formation of organic radicals, generation of peroxides, competition reactions by generated intermediates, etc. In this study a simple kinetic expression was proposed to evaluate the influence of the variables studied. Hence, the following assumptions have been accounted for. Firstly, bezafibrate is only removed by Reactive Oxygen Species (ROS) generated after PMS disproportionation by daylight. Accordingly, PMS photolysis is modelled by the expression (Doll and Frimmel, 2003):

$$-\frac{dC_{PMS}}{dt} = \phi_{\lambda,PMS} \frac{\epsilon_{\lambda,PMS} C_{PMS}}{\sum_i \epsilon_{\lambda,i} C_i} I_{\lambda,0} \left[1 - \exp(-2.303L \sum_i \epsilon_{\lambda,i} C_i) \right] \quad (2)$$

where $\phi_{\lambda,i} = \int \phi_i(\lambda) d\lambda$ is the quantum yield of the species i ; $\epsilon_{\lambda,i} = \int \epsilon_i(\lambda) d\lambda$, the extinction coefficient of the compound i ; $I_{\lambda,0} = \int \epsilon_i(\lambda) d\lambda$, the incident photon flux by the liquid in the reaction; and L , the effective optical path in the reactor.

The low PMS and BZF (and likely intermediates) extinction coefficient leads to the inequality $2.303L \sum_i \epsilon_i C_i < 0.02$. At wavelength up to 285 nm, the extinction coefficient for BZF and PMS is minimal as shown in Fig. 2. No pH influence was observed in the

1 interval of the irradiated wavelengths ($\lambda > 300$ nm). As a consequence, assuming that light
 2 is only absorbed by PMS, Eq. 2 can be transformed by expansion in Taylor series to:

$$3 \quad -\frac{dC_{PMS}}{dt} = 2.303L \phi_{\lambda, PMS} \epsilon_{\lambda, PMS} I_{\lambda, 0} C_{PMS} \quad (3)$$

4 ROS formation should be proportional to PMS depletion:

$$5 \quad \frac{dC_{ROS}}{dt} = 2.303L \phi_{\lambda, ROS} \epsilon_{\lambda, PMS} I_{\lambda, 0} C_{PMS} \quad (4)$$

6 If steady state conditions apply to ROS, bezafibrate removal can be expressed by:

$$7 \quad -\frac{dC_{BZF}}{dt} = k_{BZF} \frac{2.303L \phi_{\lambda, ROS} \epsilon_{\lambda, PMS} I_{\lambda, 0} C_{PMS}}{\Sigma r_{ROS}} C_{BZF}^n \quad (5)$$

8 where k_{BZF} is an empirical rate constant accounting for bezafibrate abatement regardless
 9 of the actual mechanism taking place, Σr_{ROS} , stands for all the reactions consuming
 10 reactive oxygenated species, and n is the empirical reaction order regarding bezafibrate
 11 oxidation.

12 Given the number of potential BZF oxidation pathways, stoichiometric coefficients,
 13 unknown rate constants, selectivity, etc., the term Σr_{ROS} is difficult to be evaluated.
 14 Obviously, the number and concentration of intermediates should be proportional to the
 15 amount of BZF oxidized. In this sense, scavenging of ROS has been incorporated to the
 16 model by the following expression:

$$17 \quad \Sigma r_{ROS} = \alpha (C_{BZF_0} - C_{BZF})^m \quad (6)$$

18 where α is the proportionality constant, the sub index “0” refers to initial conditions, and
 19 m is an adjustable reaction order concerning the oxidation of intermediates. After
 20 substitution in (5):

$$21 \quad -\frac{dC_{BZF}}{dt} = k_{Rad, BZF} \frac{2.303L \phi_{\lambda, ROS} \epsilon_{\lambda, PMS} I_{\lambda, 0} C_{PMS}}{\alpha (C_{BZF_0} - C_{BZF})^m} C_{BZF}^n \quad (7)$$

1 Finally:

$$2 \quad -\frac{dC_{\text{BZF}}}{dt} = k_{\text{Observed}} \frac{C_{\text{PMS}} C_{\text{BZF}}^n}{(C_{\text{BZF}_0} - C_{\text{BZF}})^m} \quad (8)$$

3 with

$$4 \quad k_{\text{Observed}} = k_{\text{Rad,BZF}} \frac{2.303 I_{\lambda, \text{ROS}} \phi_{\lambda, \text{ROS}} \times I_{\lambda, \text{PMS}} \phi_{\lambda, 0}}{\alpha} \quad (9)$$

5 As a rule of thumb, the evolution of PMS concentration seems to follow an exponential
6 curve from 0 to 30 min, however, its decomposition rate significantly slowed down from
7 30 min until the end of the 120 min time experiments. It is suggested that a fraction of
8 ROS initially formed are scavenged by PMS itself, however, as the concentration of
9 byproducts increases, radicals are mainly consumed by intermediates, so PMS only
10 transforms due to photolysis.

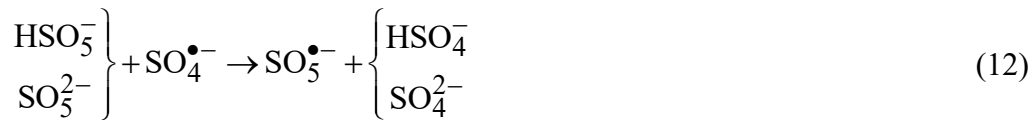
11 Experimental PMS concentration was fitted to an exponential expression of the type:

$$12 \quad C_{\text{PMS}} = C_{\text{PMS}_0} - K(1 - \exp(-\tau t)) \quad (10)$$

13 where K and τ are adjustable parameters to fit PMS experimental concentration profiles.
14 After PMS evolution fitting, Eq. 8 was numerically solved by Euler's method. Obviously,
15 Eq. 8 is a pseudoempirical model lacking of fundamental chemistry basis, however, the
16 role played by a model is the simulation of experimental data and it is just a tool to predict
17 the behavior of the system under a range of operating variable values. Optimization of
18 k_{Observed} , m and n allowed for the acceptable simulation of BZF evolution profiles at
19 different initial concentrations of the pharmaceutical. Values of $n=0.4$, $m=0.25$ and
20 $k_{\text{Observed}}=2.5 \pm 0.3 \cdot 10^{-3} \text{ M}^{-0.15} \text{ min}^{-1}$ were obtained after the optimization process when
21 Daylight was applied. Fig. 3 shows a good simulation (dashed lines) of bezafibrate
22 evolution considering that the process is not first order in this reagent.

3.2.2. Initial PMS concentration

The influence of PMS was evaluated in the interval 40-400 μM . Fig. 4 shows the results obtained. This figure reveals a positive effect of the oxidant concentration within the range of concentrations studied. The initial scavenging of radicals by PMS seems to be inevitable to form the less reactive $\text{SO}_5^{\bullet-}$ radical (eq. 11 and 12) (Rivas et al., 2012); therefore, an excessive amount of PMS could lead to experience certain inhibition of the process in terms of bezafibrate removal rate. However, under the conditions investigated in this work, this negative effect has not been experienced.



PMS conversion showed again an exponential increase in the first 30 min of reaction, regardless of the initial concentration used, as previously shown in Fig. 1B. Results suggest that there is a fixed fraction of PMS scavenging radicals within the first half an hour of the reaction independently of the initial PMS concentration used.

Once more, Eq. 8 was applied to this experimental series by keeping the values of k_{Observed} , m , and n previously obtained. As observed from Fig. 4 (dashed lines), the model was also capable of acceptably simulating the influence of PMS initial concentration on bezafibrate abatement, confirming the validity of the model.

3.2.3. pH influence

Fig. 5 shows the different curves obtained in experiments conducted under pH controlled conditions in the range 3-10. pH did not exert a significant influence in the range 3-8; however, PMS abatement increased as the pH was raised from pH 8 to pH 10.

1 Analogously, bezafibrate removal rate was also increased when pH was controlled under
2 alkaline conditions. Fig. 5 inset shows the evolution of the k_{Observed} as a function of pH.
3 As seen, in the pH range 3-8 k_{Observed} barely varies; nevertheless, at pH 9 a slight increase
4 was experienced, this trend corroborated at pH 10. Under the latter operating conditions,
5 k_{Observed} underwent a 6-fold increase if compared to values found at acidic or
6 circumneutral pH. These results are in agreement with those reported by Guan and co-
7 workers (Guan et al., 2011). These authors reported an improved efficacy of the system
8 PMS/UVC when treating an aqueous solution of benzoic acid after raising the pH from 8
9 to 12.

10 The enhancement of the oxidizing capacity is associated to an increase of the molar
11 absorptivity of PMS as this species is dissociated ($pK_a=9.5$). From Figure 2, it can be
12 appreciated that the molar extinction coefficient of the dissociated species (SO_5^-) is ten
13 times higher than the non-dissociated (HSO_5^-). For example, at 254 nm the values were
14 12.4 and 121.1 $\text{M}^{-1} \text{cm}^{-1}$, respectively.

15 3.2.4. Presence of ROS (reactive oxygenated species) scavengers

16 The influence of the reactive species involved in the process of bezafibrate oxidation
17 by photolytic activation of PMS was assessed by the application of diverse radical
18 scavengers.

19 The use of linear α -hydrogen alcohols has been proved to reliably test the influence of
20 hydroxyl and sulfate radicals. The second order rate constant for the reaction of HO^\bullet
21 increases from methanol (MeOH), ethanol (EtOH) to 2-propanol (2PrOH): $9.7 \cdot 10^8$, $(1.2-$
22 $2.8) \cdot 10^9$ and $2.8 \cdot 10^9 \text{ M}^{-1} \text{ s}^{-1}$, respectively. The reactivity of these alcohols with $\text{SO}_4^{\bullet-}$,
23 although less, is still considered high: $3.2 \cdot 10^6$, $(1.6-7.7) \cdot 10^7$ and $6 \cdot 10^7 \text{ M}^{-1} \text{ s}^{-1}$ respectively
24 for MeOH, EtOH and 2PrOH. In the case of *tert*-butyl alcohol (TBA), the second order

1 rate constant for $\text{SO}_4^{\cdot-}$ is *circa* 1000 times lower to that of HO^{\cdot} , $(3.8-7.6) \cdot 10^8$ *versus* $(4.0-$
 2 $9.1) \cdot 10^5 \text{ M}^{-1} \text{ s}^{-1}$ (Zhang et al., 2015). For that reason, the inhibition effect observed with
 3 TBA is commonly compared to linear alcohols to tentatively asses the relative importance
 4 of HO^{\cdot} and $\text{SO}_4^{\cdot-}$ in sulfate-based AOPs. Thus, linear alcohols are supposed to suppress
 5 the effect of both radicals whereas TBA is only capable of remove the effect of HO^{\cdot}
 6 efficiently. Furthermore, regardless of the values of the rate constant, it is important to
 7 take into account the concentration of the scavenger. It must be in high concentration to
 8 avoid competition with the target compound (BZF), i.e. for HO^{\cdot} :

$$9 \quad k_{\text{Scavenger}, \text{HO}^{\cdot}} \cdot C_{\text{Scavenger}} \gg \gg k_{\text{BZF}, \text{HO}^{\cdot}} \cdot C_{\text{BZF}} \quad (13)$$

10 The influence of these alcohols in the degradation of BZF by solar-assisted PMS
 11 oxidation was tested at different pH values (3, 5, 7, 9) and Fig. 6 depicts the results. The
 12 rate constant of BZF and hydroxyl radicals is around $8 \cdot 10^9 \text{ M}^{-1} \text{ s}^{-1}$ (Razavi et al., 2009);
 13 therefore under the experimental conditions (5 mM alcohol and 2.76 μM BZF), all
 14 alcohols can be considered scavengers of HO^{\cdot} route. Specifically, as an example, the
 15 calculated k_{Observed} values at pH=3 indicated a 63.8% and 72.5% reduction if compared to
 16 the non-scavenged run, for TBA and EtOH, respectively. At pH=7 (Fig. 6 left down), the
 17 inhibition of the process by linear alcohols was enhanced if compared to pH 3 and 5,
 18 generally accompanied by a higher PMS decomposition rate. The scavenging effect
 19 followed the order $\text{PrOH} > \text{EtOH} > \text{MeOH}$, which agrees with the decreasing order of their
 20 rate constant values with HO^{\cdot} and $\text{SO}_4^{\cdot-}$ (Neta et al., 1988). As pH increased from 3 to 9,
 21 a higher consumption of PMS was registered, probably due to the formation of active
 22 organic radicals (Rivas et al., 2015). The role played by $\text{SO}_4^{\cdot-}$ versus HO^{\cdot} loses
 23 importance if compared to hydroxyl radical as pH is raised. Actually, at pH=9 the
 24 presence of TBA did not affect the BZF removal profile if compared to the blank.

1 According to the literature, p-benzoquinone (pBZQ) has been used to check the role
2 played by superoxide radical, second order rate constant of pBZQ and the pair $\text{HO}_2^\bullet/\text{O}_2^\bullet$
3 $(0.9\text{--}1.0)\cdot 10^9 \text{ M}^{-1} \text{ s}^{-1}$ (Yang et al., 2018). Addition of pBZQ significantly affected the
4 process. Almost a 93% decrease in k_{Observed} was found at $\text{pH}=3$, if compared to the studies
5 in absence of scavengers. Although benzoquinone is used as a $\text{HO}_2^\bullet/\text{O}_2^\bullet$ scavenger, the
6 reaction rate constant with HO^\bullet is even higher, $6.6\cdot 10^9 \text{ M}^{-1} \text{ s}^{-1}$ (Nien Schuchmann et al.,
7 1998). Furthermore, pBZQ also reacts with sulfate radicals, $10^8 \text{ M}^{-1} \text{ s}^{-1}$ (Neta et al., 1988).
8 Therefore, pBZQ should be capable to quench the three radicals; nevertheless, this was
9 not the case. A parallel scavenging effect does likely proceed. A plausible explanation
10 could be an important role played by hydroperoxyl radicals; however, this is not likely to
11 occur since the reactivity of this kind of radicals with BZF is lower than the corresponding
12 HO^\bullet and SO_4^\bullet radicals. Competition by light seems to be a more reasonable explanation.
13 Hence, benzoquinone absorbs light from UVC to the visible region of the spectrum, i.e.
14 $\epsilon_{300\text{nm}} < 30 \text{ m}^2 \text{ mol}^{-1}$ (von Sonntag et al., 2004). In this case, light competition should lead
15 to a lower PMS conversion; nevertheless, PMS abatement extent is higher when pBZQ is
16 present. Accordingly, inefficient PMS decomposition by pBZQ is hypothesized. In this
17 sense, Zhou and co-workers (Zhou et al., 2015) proposed a non-radical mechanism of
18 PMS reaction with benzoquinone to generate $^1\text{O}_2$ through a dioxirane intermediate.
19 Apparently, $^1\text{O}_2$ would not contribute to bezafibrate oxidation so the presence of pBZQ
20 involves a negative effect in this particular case. Previous results were confirmed at $\text{pH}=5$
21 (Fig. 6, top right) where the inefficient PMS decomposition by pBZQ was more evident.

22 **3.3. Intermediates identification and toxicity**

23 In this work, 11 initial intermediates were identified when treating bezafibrate with the
24 system PMS/Daylight, as summarized in Table 3. In addition, Fig. 7 shows the proposed
25 reaction mechanism in which, six potential routes of bezafibrate attack are proposed. The

1 first one is the addition of HO• to one of the aromatic rings leading to C6; also attack to
2 the Cl group results in the dechlorinated species C11. Removal of the acidic group to
3 generate C9 would also sustain the detection of formic acid early in the process. The
4 registered peak area can be considered proportional to concentration in all the
5 intermediates in similar extent; therefore, the formation of C7 from C9 seems to be the
6 preferential route at the sight of Fig. 8B. Attack to the amine group would break the
7 bezafibrate structure to give C3 and C8. C1 structure would be the result of ring opening
8 while the unusual C5 can be explained by cyclization after hydrogen abstraction by HO•.
9 Some of the intermediates detected have also been reported previously. Hence Razavi and
10 co-workers (Razavi et al., 2009) propose a four route bezafibrate oxidation identifying
11 compounds C2, C4, C5, C6, C7 and C11. These authors propose a scheme to account for
12 the cyclization product C5.

13 The evolution of some carboxylic acids and intermediates was also monitored.
14 Muconic acid was detected evidencing the opening of the aromatic ring. Muconic acid
15 likely leads to formation of fumaric acid and further accumulation of formic acid. At the
16 end of the process (120 min), roughly 26% of the maximum stoichiometric amount of
17 free chlorides was detected in the water bulk (results not shown).

18 Toxicity of first intermediates was theoretically evaluated by using TEST®, a Toxicity
19 Estimation Software Tool developed to estimate the toxicity of chemicals using
20 Quantitative Structure Activity Relationships (QSARs) methodologies (Martin, 2016).
21 Four different parameters were evaluated, namely, *fat minnow* LC50 (96h), *Daphnia*
22 *Magna* LC50 (48h), *Tetrahymena Pyriformis* IGC50 (48h) and oral rat LD50. Fig. 8A
23 illustrates the relative toxicity of the intermediates if compared to bezafibrate toxicity. As
24 observed, most of intermediates show a lower toxicity than the parent compound.
25 Nevertheless, intermediates, C4-C6 and C9 seems to be more toxic than bezafibrate. As

1 a rule of thumb, substances keeping the chloro-substituent present a higher negative effect
2 in terms of toxicity, especially when the structure of the molecule has not been
3 significantly modified if compared to bezafibrate chemical structure. In any case, under
4 the conditions investigated, only C10 seems to accumulate in the water bulk, the rest of
5 intermediates show a decreasing concentration trend as the reaction progresses (see Fig.
6 8B). The experiment conducted to identify the intermediates was carried out with an
7 initial BZF concentration of 10 mg L^{-1} , accordingly, it is expected that at lower BZF doses
8 most of intermediates are completely removed after 120 min of treatment.

9 **3.4. A case of study: removal of bezafibrate in a simulated secondary effluent**

10 In order to prove the feasibility of solar photolytic-PMS technology, a series of
11 experiments of BZF oxidation in a matrix simulating the effluent of a wastewater
12 treatment plant after the biological oxidation was conducted. Fig. 9A shows the evolution
13 of the normalized BZF concentration during the treatment with PMS photolysis using the
14 three radiation filters. From the results, BZF removal was less efficient in the Synthetic
15 Urban WasteWater (SUWW) matrix if compared to ultrapure water. Actually, under the
16 conditions tested (BZF initial concentration, $250 \text{ } \mu\text{g L}^{-1}$; PMS $400 \text{ } \mu\text{M}$) the most energetic
17 radiation, i.e. Daylight, almost 85% elimination of the target pollutant was achieved in 2
18 hours. It was necessary to raise the initial PMS concentration to $800 \text{ } \mu\text{M}$ to achieve a
19 complete degradation of BZF. Also, the the UVC content in the radiation source played
20 an important role in the SUWW. PMS photolysis with Windowglass radiation achieved
21 only 20% BZF removal and Storelight was completely inefficient. Taking in mind the
22 positive effectiveness in ultrapure water, the competition of substances in SUWW, either
23 organic or inorganic, and BZF for the generated radicals diminished the efficacy of the
24 process. Only the Daylight radiation was capable of triggering the generation of enough
25 oxidizing radicals to perform BZF degradation. Moreover, the kinetics of the process in

1 SUWW matrix is completely different to what appreciated in ultrapure water. In presence
2 of SUWW, BZF follows a zero order kinetics at initial PMS dose of 400 μM . That may
3 indicate that the amount of free radicals available for BZF oxidation is limiting the
4 process. Higher initial PMS concentration led to exponential decay.

5 In order to compare ultrapure (UP) and SUWW matrices, the initial rate constant for
6 the observed BZF depletion ($r_{\text{BZF},0}$) during the different systems used are presented in Fig.
7 9B. The $r_{\text{BZF},0}$ in UP water was obtained from experimental results obtained in Fig. 1B.
8 As it can be appreciated, $r_{\text{BZF},0}$ in SUWW matrix was over 2 orders of magnitude inferior
9 to what registered in UP, even though the molar ratio PMS:BZF in those experiments was
10 higher to UP tests. These results reveal the importance of considering the competitors
11 present in real water matrix in order to select the PMS initial dose in the design of real
12 treatment applications.

13 4. CONCLUSIONS

14 The combination of PMS and solar radiation results in effective removal of organic
15 contaminants as shown in the case of bezafibrate and the intermediate products. Solar
16 radiation, which contains some small portion of UV radiation demonstrates to be effective
17 in the activation of PMS for the oxidation of aqueous micropollutants, i.e. bezafibrate.
18 The UV proportion in the irradiation source seems to be limiting in the process, with a
19 higher effectiveness of $\text{UVC} > \text{UVB} > \text{UVA}$ components. Experimental obtained in this
20 study reveal a reaction order different from 1 regarding bezafibrate oxidation and close
21 to 1 in the case of PMS degradation. The use of scavengers suggests the presence of
22 radicals, the role played by HO^\bullet being prevailing that of $\text{SO}_4^{\bullet-}$ with the increase in pH in
23 the alkaline range. Eleven transformation products were detected at the beginning of the
24 bezafibrate oxidation by PMS and solar light. Stoichiometric amounts of free chloride
25 determined after roughly 30 min of reaction suggests the dechlorination route of

1 bezafibrate removal as the main pathway. In experiments using wastewater matrix, it is
2 necessary to increase the ratio oxidant-pollutant to achieve degradation similar rates to
3 those obtained in ultrapure water.

4 **Acknowledgements**

5 Rafael Rodríguez Solís is grateful to *Ramón Areces* foundation for his postdoctoral
6 fellowship in the University of Cincinnati (*XXX edition of grants for postgraduate studies*
7 *in Life and Matter Sciences in foreign universities and research centers*). Authors also
8 acknowledge the '*Servicio de Análisis Elemental y Molecular (SAEM)* of *Servicios de*
9 *Apoyo a la Investigación de la Universidad de Extremadura (SAIUex)*' for the help and
10 guidance with the intermediate products analyses.

11 **References**

- 12 Ao, X., Liu, W., 2017. Degradation of sulfamethoxazole by medium pressure UV and
13 oxidants: Peroxymonosulfate, persulfate, and hydrogen peroxide. *Chem. Eng. J.* 313,
14 629–637. [https://doi.org/https://doi.org/10.1016/j.cej.2016.12.089](https://doi.org/10.1016/j.cej.2016.12.089)
- 15 Beltrán, J.F., Rey, A., 2017. Solar or UVA-Visible Photocatalytic Ozonation of Water
16 Contaminants. *Molecules*. <https://doi.org/10.3390/molecules22071177>
- 17 Bletsou, A.A., Jeon, J., Hollender, J., Archontaki, E., Thomaidis, N.S., 2015. Targeted
18 and non-targeted liquid chromatography-mass spectrometric workflows for
19 identification of transformation products of emerging pollutants in the aquatic
20 environment. *TrAC Trends Anal. Chem.* 66, 32–44.
21 <https://doi.org/10.1016/J.TRAC.2014.11.009>
- 22 Christou, A., Agüera, A., Bayona, J.M., Cytryn, E., Fotopoulos, V., Lambropoulou, D.,
23 Manaiá, C.M., Michael, C., Revitt, M., Schröder, P., Fatta-Kassinos, D., 2017. The
24 potential implications of reclaimed wastewater reuse for irrigation on the agricultural
25 environment: The knowns and unknowns of the fate of antibiotics and antibiotic
26 resistant bacteria and resistance genes – A review. *Water Res.* 123, 448–467.
27 <https://doi.org/10.1016/J.WATRES.2017.07.004>

- 1 Daughton, C.G., Ternes, T.A., 1999. Pharmaceuticals and personal care products in the
2 environment: agents of subtle change? *Environ. Health Perspect.* 107, 907–938.
3 <https://doi.org/10.1289/ehp.99107s6907>
- 4 Doll, T.E., Frimmel, F.H., 2003. Fate of pharmaceuticals—photodegradation by
5 simulated solar UV-light. *Chemosphere* 52, 1757–1769.
6 [https://doi.org/10.1016/S0045-6535\(03\)00446-6](https://doi.org/10.1016/S0045-6535(03)00446-6)
- 7 Erdei, L., Arecrachakul, N., Vigneswaran, S., 2008. A combined photocatalytic slurry
8 reactor–immersed membrane module system for advanced wastewater treatment.
9 *Sep. Purif. Technol.* 62, 382–388. <https://doi.org/10.1016/J.SEPPUR.2008.02.003>
- 10 EU, E.C., 2003. Technical Guidance Document on Risk assessment (TGD) in support of
11 Commission Directive 93/67/ECC, in: Commission Regulation (EC) No 1488/94
12 and Directive 98/8/EC. Ispra, Italy.
- 13 Fent, K., Weston, A.A., Caminada, D., 2006. Ecotoxicology of human pharmaceuticals.
14 *Aquat. Toxicol.* 76, 122–159. <https://doi.org/10.1016/J.AQUATOX.2005.09.009>
- 15 Fukushima, M., Tatsumi, K., 2005. Effect of Hydroxypropyl- β -cyclo- dextrin on the
16 Degradation of Pentachlorophenol by Potassium Monopersulfate Catalyzed with
17 Iron(III)–Porphyrin Complex. *Environ. Sci. Technol.* 39, 9337–9342.
18 <https://doi.org/10.1021/es051355r>
- 19 Ghanbari, F., Moradi, M., 2017. Application of peroxymonosulfate and its activation
20 methods for degradation of environmental organic pollutants: Review. *Chem. Eng.*
21 *J.* 310, 41–62. <https://doi.org/https://doi.org/10.1016/j.cej.2016.10.064>
- 22 Goldstein, S., Rabani, J., 2008. The ferrioxalate and iodide–iodate actinometers in the UV
23 region. *J. Photochem. Photobiol. A Chem.* 193, 50–55.
24 <https://doi.org/10.1016/J.JPHOTOCHEM.2007.06.006>
- 25 Guan, Y.-H., Ma, J., Li, X.-C., Fang, J.-Y., Chen, L.-W., 2011. Influence of pH on the
26 Formation of Sulfate and Hydroxyl Radicals in the UV/Peroxymonosulfate System.
27 *Environ. Sci. Technol* 45, 30. <https://doi.org/10.1021/es2017363>
- 28 Jones, P.H., 2009. CHAPTER 26 - Fibrates, in: Ballantyne, C.M.B.T.-C.L. (Ed.), . W.B.
29 Saunders, Philadelphia, pp. 315–325. [https://doi.org/https://doi.org/10.1016/B978-](https://doi.org/https://doi.org/10.1016/B978-141605469-6.50030-5)
30 [141605469-6.50030-5](https://doi.org/https://doi.org/10.1016/B978-141605469-6.50030-5)

- 1 Liu, J., Zhao, Z., Shao, P., Cui, F., 2015. Activation of peroxy monosulfate with magnetic
2 Fe₃O₄-MnO₂ core-shell nanocomposites for 4-chlorophenol degradation. *Chem.*
3 *Eng. J.* 262, 854–861. <https://doi.org/10.1016/j.cej.2014.10.043>
- 4 Martin, T. (National R.M.R.E., 2016. User's Guide for T.E.S.T. (version 4.2) (Toxicity
5 Estimation Software Tool) A Program to Estimate Toxicity from Molecular
6 Structure. US Environmental Protection Agency, Cincinnati (Ohio).
- 7 Matafonova, G., Batoev, V., 2018. Recent advances in application of UV light-emitting
8 diodes for degrading organic pollutants in water through advanced oxidation
9 processes: A review. *Water Res.* 132, 177–189.
10 <https://doi.org/10.1016/j.watres.2017.12.079>
- 11 Neta, P., Huie, R.E., Ross, A.B., 1988. Rate Constants for Reactions of Inorganic Radicals
12 in Aqueous Solution. *J. Phys. Chem. Ref. Data* 17, 1027–1284.
13 <https://doi.org/10.1063/1.555808>
- 14 Nien Schuchmann, M., Bothe, E., von Sonntag, J., von Sonntag, C., 1998. Reaction of
15 OH radicals with benzoquinone in aqueous solutions. A pulse radiolysis study. *J.*
16 *Chem. Soc. Perkin Trans. 2* 791–796. <https://doi.org/10.1039/A708772A>
- 17 Razavi, B., Song, W., Cooper, W.J., Greaves, J., Jeong, J., 2009. Free-Radical-Induced
18 Oxidative and Reductive Degradation of Fibrate Pharmaceuticals: Kinetic Studies
19 and Degradation Mechanisms. *J. Phys. Chem. A* 113, 1287–1294.
20 <https://doi.org/10.1021/jp808057c>
- 21 Rivas, F.J., Gimeno, O., Borallho, T., 2012. Aqueous pharmaceutical compounds
22 removal by potassium monopersulfate. Uncatalyzed and catalyzed semicontinuous
23 experiments. *Chem. Eng. J.* 192, 326–333.
24 <https://doi.org/10.1016/J.CEJ.2012.03.055>
- 25 Solís, R.R., Rivas, F.J., Tierno, M., 2016. Monopersulfate photocatalysis under 365 nm
26 radiation. Direct oxidation and monopersulfate promoted photocatalysis of the
27 herbicide tembotrione. *J. Environ. Manage.* 181, 385–394.
28 <https://doi.org/10.1016/J.JENVMAN.2016.06.061>
- 29 STATISTA, n.d. Global Pharmaceutical Industry - Statistics & Facts [WWW Document].
30 Stat. Doss. about Glob. Pharm. Ind.

- 1 Sui, Q., Yan, P., Cao, X., Lu, S., Zhao, W., Chen, M., 2016. Biodegradation of bezafibrate
2 by the activated sludge under aerobic condition: Effect of initial concentration,
3 temperature and pH. *Emerg. Contam.* 2, 173–177.
4 <https://doi.org/https://doi.org/10.1016/j.emcon.2016.09.001>
- 5 Tamura, H., Goto, K., Yotsuyanagi, T., Nagayama, M., 1974. Spectrophotometric
6 determination of iron(II) with 1,10-phenanthroline in the presence of large amounts
7 of iron(III). *Talanta* 21, 314–318. [https://doi.org/10.1016/0039-9140\(74\)80012-3](https://doi.org/10.1016/0039-9140(74)80012-3)
- 8 von Sonntag, J., Mvula, E., Hildenbrand, K., von Sonntag, C., 2004. Photohydroxylation
9 of 1,4-Benzoquinone in Aqueous Solution Revisited. *Chem. – A Eur. J.* 10, 440–
10 451. <https://doi.org/10.1002/chem.200305136>
- 11 Waclawek, S., Lutze, H. V., Grübel, K., Padil, V.V.T., Černík, M., Dionysiou, D.D.,
12 2017. Chemistry of persulfates in water and wastewater treatment: A review. *Chem.*
13 *Eng. J.* 330, 44–62. <https://doi.org/10.1016/J.CEJ.2017.07.132>
- 14 Wang, J., Wang, S., 2018. Activation of persulfate (PS) and peroxymonosulfate (PMS)
15 and application for the degradation of emerging contaminants. *Chem. Eng. J.* 334,
16 1502–1517. <https://doi.org/https://doi.org/10.1016/j.cej.2017.11.059>
- 17 Yang, S., Wu, P., Liu, J., Chen, M., Ahmed, Z., Zhu, N., 2018. Efficient removal of
18 bisphenol A by superoxide radical and singlet oxygen generated from
19 peroxymonosulfate activated with Fe⁰-montmorillonite. *Chem. Eng. J.* 350, 484–
20 495. <https://doi.org/https://doi.org/10.1016/j.cej.2018.04.175>
- 21 Zhang, B.-T., Zhang, Y., Teng, Y., Fan, M., 2015. Sulfate Radical and Its Application in
22 Decontamination Technologies. *Crit. Rev. Environ. Sci. Technol.* 45, 1756–1800.
23 <https://doi.org/10.1080/10643389.2014.970681>
- 24 Zhou, Y., Jiang, J., Gao, Y., Ma, J., Pang, S.-Y., Li, J., Lu, X.-T., Yuan, L.-P., 2015.
25 Activation of Peroxymonosulfate by Benzoquinone: A Novel Nonradical Oxidation
26 Process. *Environ. Sci. Technol.* 49, 12941–12950.
27 <https://doi.org/10.1021/acs.est.5b03595>